





# Metabolic abnormalities and reprogramming in cats with naturally occurring hypertrophic cardiomyopathy

Qinghong Li<sup>1\*</sup> , Max Homilius<sup>2</sup>, Erin Achilles<sup>3</sup>, Laura K. Massey<sup>3</sup>, Victoria Convey<sup>3</sup>, Åsa Ohlsson<sup>4</sup> , Ingrid Ljungvall<sup>5</sup> , Jens Häggström<sup>5</sup> , Brittany Vester Boler<sup>1</sup>, Pascal Steiner<sup>1</sup>, Sharlene Day<sup>6</sup>, Calum A. MacRae<sup>2\*</sup> and Mark A. Oyama<sup>3\*</sup>

<sup>1</sup>Nestlé Purina Research, St. Louis, Missouri, USA; <sup>2</sup>Brigham and Women's Hospital and Harvard Medical School, Boston, Massachusetts, USA; <sup>3</sup>Department of Clinical Sciences and Advanced Medicine, University of Pennsylvania, Philadelphia, Pennsylvania, USA; <sup>4</sup>Department of Animal Biosciences, Swedish University of Agricultural Sciences, Uppsala, Sweden; <sup>5</sup>Department of Clinical Sciences, Swedish University of Agricultural Sciences, Uppsala, Sweden; and <sup>6</sup>Division of Cardiovascular Medicine, Perelman School of Medicine, University of Pennsylvania, Philadelphia, Pennsylvania, USA

## Abstract

**Background and aims** The heart is a metabolic organ rich in mitochondria. The failing heart reprograms to utilize different energy substrates, which increase its oxygen consumption. These adaptive changes contribute to increased oxidative stress. Hypertrophic cardiomyopathy (HCM) is a common heart condition, affecting approximately 15% of the general cat population. Feline HCM shares phenotypical and genotypical similarities with human HCM, but the disease mechanisms for both species are incompletely understood. Our goal was to characterize global changes in metabolome between healthy control cats and cats with different stages of HCM.

**Methods** Serum samples from 83 cats, the majority (70/83) of which were domestic shorthair and included 23 healthy control cats, 31 and 12 preclinical cats with American College of Veterinary Internal Medicine (ACVIM) stages B1 and B2, respectively, and 17 cats with history of clinical heart failure or arterial thromboembolism (ACVIM stage C), were collected for untargeted metabolomic analysis. Multiple linear regression adjusted for age, sex and body weight was applied to compare between control and across HCM groups.

**Results** Our study identified 1253 metabolites, of which 983 metabolites had known identities. Statistical analysis identified 167 metabolites that were significantly different among groups (adjusted  $P < 0.1$ ). About half of the differentially identified metabolites were lipids, including glycerophospholipids, sphingolipids and cholesterol. Serum concentrations of free fatty acids, 3-hydroxy fatty acids and acylcarnitines were increased in HCM groups compared with control group. The levels of creatine phosphate and multiple Krebs cycle intermediates, including succinate, aconitate and  $\alpha$ -ketoglutarate, also accumulated in the circulation of HCM cats. In addition, serum levels of nicotinamide and tryptophan, precursors for de novo NAD<sup>+</sup> biosynthesis, were reduced in HCM groups versus control group. Glutathione metabolism was altered. Serum levels of cystine, the oxidized form of cysteine and cysteine-glutathione disulfide, were elevated in the HCM groups, indicative of heightened oxidative stress. Further, the level of ophthalmate, an endogenous glutathione analog and competitive inhibitor, was increased by more than twofold in HCM groups versus control group. Finally, several uremic toxins, including guanidino compounds and protein bound putrescine, accumulated in the circulation of HCM cats.

**Conclusions** Our study provided evidence of deranged energy metabolism, altered glutathione homeostasis and impaired renal uremic toxin excretion. Altered lipid metabolism suggested perturbed structure and function of cardiac sarcolemma membrane and lipid signalling.

**Keywords** feline; glutathione; energy metabolism; NAD; uremic toxin; lipid

Received: 21 May 2024; Revised: 15 September 2024; Accepted: 5 October 2024

\*Correspondence to: Qinghong Li, Nestlé Purina Research, Checkerboard Square 2RS, St. Louis, MO 63164, USA. Email: qinghong.li@rd.nestle.com

Calum A. MacRae, Brigham and Women's Hospital and Harvard Medical School, Boston, Massachusetts, USA. Email: cmacrae@bwh.harvard.edu

Mark A. Oyama, Department of Clinical Sciences and Advanced Medicine, University of Pennsylvania, Philadelphia, Pennsylvania, USA. Email: maoyama@vet.upenn.edu

Calum A. MacRae and Mark A. Oyama contributed equally to the study.

**Funding information:** The study was funded by the Nestlé Purina PetCare Company.

## Introduction

Hypertrophic cardiomyopathy (HCM) is the most prevalent heart disease in cats, affecting 10%–15% the general pet cat population.<sup>1–3</sup> The disease is characterized by increased myocardial thickening associated with hypertrophic non-dilated left ventricle.<sup>4</sup> The prevalence of HCM in the UK shelter cats increases with age, with approximately 30% cats aged 9 years or older affected.<sup>2</sup> Recent consensus statements of American College of Veterinary Internal Medicine (ACVIM) provided up-to-date guidelines for classification and diagnosis of cardiomyopathy in cats.<sup>5</sup> Cats in stage A are predisposed to cardiomyopathy with no evidence of myocardial disease. Stage B refers to preclinical cats, which have echocardiographic evidence of cardiomyopathy, but without clinical signs such as laboured or rapid breathing and lethargy. Stage B is further divided into two substages by means of atrial dimensions, B1 with lower risk of imminent congestive heart failure (CHF) or arterial thromboembolism (ATE), while B2 with higher risk of imminent CHF or ATE. Cats with history of clinical CHF or ATE are classified as stage C. A majority of the cats with HCM remain preclinical with prolonged stage B, with a 5 year cumulative incidence of cardiac mortality of approximately 23% while 30% developed clinical signs of CHF or ATE or both.<sup>5,6</sup> Feline HCM has been shown to result from mutations in the *MYPBC3* gene in Maine Coon and Ragdoll cats although a substantial fraction of affected cats have no evidence of mutation in any of the genes implicated in the HCM.<sup>7,8</sup>

The heart is a metabolically active organ with a higher resting metabolic rate and mitochondrial abundance than any other organs.<sup>9–11</sup> Energy deficiency plays a central role in the development of heart failure (HF).<sup>12</sup> In the adult mammalian heart, mitochondrial fatty acid (FA) oxidation (FAO) contributes to 70%–90% of the adenosine triphosphate (ATP) production.<sup>13–16</sup> Mitochondrial oxidative respiration contributes to approximately 90% of cellular reactive oxygen species (ROS).<sup>17,18</sup>

The failing heart experiences increased inefficiency of FAO, reprograms to utilize alternative energy substrates, which increase its oxygen consumption. This adaptive response contributes to the generation of ROS.<sup>19–22</sup> In excess, ROS can induce oxidative damage, leading to further mitochondrial dysfunction and cell death.<sup>23</sup> In the normal physiological conditions, cardiomyocytes finely regulate mitochondrial ROS homeostasis with an array of antioxidant systems, several of which depend on glutathione.<sup>18</sup>

Glutathione, a tripeptide composed of glycine, cysteine and glutamate, is a central antioxidant in cells. In the normal cytosolic environment, glutathione primarily exists in its reduced form (GSH), one of the key scavengers of ROS, with a small amount of oxidized disulfide form (GSSG). The ratio of GSH/GSSG serves as an indicator of oxidative stress.<sup>24</sup> Under heightened oxidative stress, a significant percentage of

GSH is oxidized to GSSG, leading to a decreased ratio of GSH/GSSG. In humans and pets, cardiac disease is known to be associated with mitochondrial oxidative stress, a decreased GSH/GSSG ratio, and an inability to restore normal GSH levels.<sup>25–28</sup>

Multi-omics approaches, including metabolomics, transcriptomics and proteomics, have been applied to study human HCM and numerous molecular signatures and metabolic alterations were identified.<sup>29–32</sup> In cats, serum proteomics studies comparing expressions of circulating proteins and a myocardial transcriptomics study comparing tissue gene expressions between healthy cats and cats with HCM were reported.<sup>33–35</sup> Mutations in sarcomeric protein-coding genes have been identified in humans and Maine Coon and Ragdoll cats with HCM.<sup>36–38</sup> To our knowledge, this is the first metabolomics study in feline HCM. Our goal was to characterize global metabolome changes in different stages of HCM versus healthy controls, to gain insights into the metabolic landscape of feline HCM, and to generate hypotheses for future studies. Naturally occurring HCM in cats shares genotypical and phenotypical similarities to human HCM and is considered a model for human HCM.<sup>39</sup> Cats have a shorter life span than people. Learning from cats may be applied to improve heart health in both species.

## Methods

### Animals and study approval

Eighty-three domestic cats from private homes were enrolled, included 23 cats with ACVIM stage A as the healthy control group, 31 and 12 cats with ACVIM stage B1 and B2 HCM respectively, and 17 cats with a history of CHF or ATE secondary to HCM (stage C) (*Table 1*). The study protocol was approved by the Institutional Animal Care and Use Committees of University of Pennsylvania and Nestlé Purina PetCare Company. Informed owner consents were obtained from the pet owners.

### Serum sample collection

Venous blood samples of 2–3 mL were collected in plain red-topped tubes. The blood was allowed to clot and centrifuged at 1600 *g* for 5 min to yield serum samples, which were stored at –80°C until use.

### Blood pressure, echocardiography and HCM classification

Systolic blood pressure was measured using Doppler sphygmomanometry. Echocardiographic studies (iE33, Philips

**Table 1** Physical and clinical descriptions of cats.

ACVIM group	A	B1	B2	C	P value
Sample size	23	31	12	17	
Sex (F/M)	11/12	7/24	1/11	6/11	0.071
Age (year)	6.5 ± 0.8	9.1 ± 0.7	7.9 ± 1.3	7.5 ± 1.0	0.14
Weight (kg)	4.7 ± 0.2	5.6 ± 0.3	5.3 ± 0.3	5.4 ± 0.3	0.065
Breed					
DSH	21	24	10	15	
DLH	0	3	0	1	
British SH	1	1	0	0	
Cornish Rex	1	0	0	0	
Russian Blue	0	1	1	0	
Scottish Fold	0	1	0	0	
Siamese	0	0	1	0	
Sphynx	0	1	0	1	
Blood pressure and echocardiography*					
BP (mmHg)	127 ± 6	135 ± 4	129 ± 6	120 ± 5	0.17
LVIDd (cm)	1.5 ± 0.0	1.5 ± 0.0	1.6 ± 0.1	1.5 ± 0.1	0.58
LVIDs (cm)	0.7 ± 0.1	0.7 ± 0.0	0.8 ± 0.1	0.8 ± 0.1	0.14
IVSd (cm)	0.5 ± 0.0	0.6 ± 0.0	0.6 ± 0.0	0.7 ± 0.1	0.018
LVPWd (cm)	0.4 ± 0.0 <sup>a</sup>	0.6 ± 0.0 <sup>ab</sup>	0.7 ± 0.0 <sup>b</sup>	0.7 ± 0.1 <sup>b</sup>	0.006
LAD (cm)	1.1 ± 0.0 <sup>a</sup>	1.3 ± 0.0 <sup>a</sup>	1.8 ± 0.1 <sup>b</sup>	1.9 ± 0.1 <sup>b</sup>	<0.0001
LA:Ao	1.2 ± 0.1 <sup>a</sup>	1.3 ± 0.0 <sup>a</sup>	1.7 ± 0.1 <sup>b</sup>	1.9 ± 0.1 <sup>b</sup>	<0.0001

Note: All cats were neutered. *P* value for continuous variables was obtained from ANOVA test while *P* value for sex was obtained from Fisher's exact test. Continuous variables are expressed as mean ± SEM. Different superscript letters indicate that there is a significant difference between groups while the same letters indicate no significant difference.

Abbreviations: BP, systolic blood pressure; DLH, domestic long-haired; DSH, domestic short-haired; IVSd, interventricular septum thickness end diastole; LA: Ao, left atrial to aortic root ratio; LAD, left atrial diameter; LVIDd, left ventricular internal diameter end diastole; LVIDs, left ventricular internal diameter end systole; LVPWd, left ventricle posterior wall thickness end diastole.

\*In group A, only five and six cats had BP and echocardiography measurements, respectively.

Healthcare) were performed without sedation. Left ventricular internal dimensions in end-diastole and left ventricular internal dimensions in end-systole, normalized left atrial diameter (nLAD) and normalized aortic root diameter were measured from right parasternal short-axis two-dimensional images and normalized to body weight. The ratio of the left atrial (LA) diameter (LAD) to the aortic root diameter was calculated. Diagnosis and staging of cats were performed by the board-certified veterinary cardiologists based on clinical and echocardiographic data. Clinically healthy cats without a heart murmur and without concurrent systemic disease were prospectively enrolled as controls (group A). This group of cats primarily consisted of systemically healthy cats owned by students and staff of the hospital. A cohort of cats with a left apical systolic murmur, echocardiographic diagnosis of thickened left ventricles, as well as clinical history and physical examination consistent with stage B1, B2 or C HCM, as described in Fuentes et al., were considered for group B1, group B2 and group C, respectively. Briefly, for the majority of normal-sized cats, an end-diastolic left ventricular (LV) wall thickness (LVPWd) ≥ 6 mm in the absence of systemic hypertension or hyperthyroidism is indicative of hypertrophy, while LVPWd ≤ 5 mm is considered normal. LVPWd between 5 and 6 mm should be interpreted in the context of body size, family history, qualitative assessment of LA and LV morphology and function, presence of dynamic LV outflow tract obstruction and tissue Doppler imaging velocities.<sup>5</sup> In this study, en-

larged left atrium forms the basis of differentiating between stage B1 and stage B2, using LA to aortic root ratio (LA: Ao) = 1.7 as the dividing line. Any cat with severe concurrent systemic disease including diabetes mellitus, cancer or kidney disease, or those with any congenital heart disease, was excluded.

## Metabolomics

Untargeted metabolomics assays were performed at a commercial laboratory (Metabolon, Inc.). Sample preparation and extraction, liquid chromatography, and mass spectrometry followed Metabolon standard protocols as previously described (Supporting information Methods).<sup>40,41</sup> Compound detection and identification were performed using Metabolon proprietary software and database. A total of 1253 biochemicals were identified, including 983 named chemicals and 270 compounds of unknown structural identity.

## Batch normalization, imputation and transformation

The raw data are unnormalized peak areas known as the area-under-the-curve calculated using ion counts to provide

relative quantification (Supporting information S1). For each metabolite, the raw values in the experimental samples are divided by the median of those samples in each instrument batch, giving each batch and thus the metabolite a median of one. Missing metabolite values in an untargeted metabolomic data can typically be attributed to the signal falling below the limit of detection. For each metabolite, we replaced missing values with its observed minimum after batch normalization. The batch-normalized and imputed data were transformed using the natural logarithm. Metabolites that had a zero standard deviation were excluded.

## Statistical analysis

Multiple linear regression adjusted for age, sex and body weight was performed to identify differential metabolites. *P* values of the regression model were adjusted to control the false discovery rate (FDR) using the Benjamini–Hochberg method.<sup>42</sup> Metabolites were then subjected to Tukey's post hoc multiple tests where the family-wise error rate was controlled. Because  $FDR < 0.05$  has been suggested as being too restrictive for many clinical settings to embrace all potential meaningful changes, less restricted statistical approaches are relevant in hypothesis-generating studies, especially in metabolomics where most studies do not have flux data despite the high coefficients of variance for resting measurement.<sup>43,44</sup> Metabolites were considered significant if FDR for the model was  $< 0.1$  and the adjusted *P* value from at least one of the multiple comparisons was  $< 0.05$ .

Principal component (PC) analysis (PCA) was performed using MetaboAnalyst 6.0. The first two PCs, PC1 and PC2, which captured more data variations than other PCs, were examined for their ability to separate the groups. Multiple linear regression using PC1 or PC2 as the dependent variable and group as the independent variable, adjusted for age, sex, and body weight was performed. The *P* values were adjusted for multiple testing error using FDR. Tukey's post hoc test was performed to compare the means between groups.

To compare the means of continuous variables among multiple groups, ANOVA and Tukey's post hoc tests were performed, and the multiple testing error was adjusted. To compare the means between two groups, Student's *t* test was used instead. To test the null hypothesis that the two categorical variables were independent,  $\chi^2$  test was performed if all expected numbers were greater than five. Otherwise, Fisher's exact test was used instead. *P* value less than 0.05 ( $P < 0.05$ ) was considered significant. Fold change was calculated as the ratio of two group means.

Data processing, analysis and presentation were performed using the statistical computing software R (version 4.3.2), MetaboAnalyst and GraphPad Prism (version 10.2.2).

## Results

### Clinical characteristics

Eighty-three privately owned cats, including 23 cats with ACVIM stage A as healthy control (group A), 31 and 12 cats with ACVIM stages B1 and B2 HCM (groups B1 and B2), respectively and 17 cats with history of CHF or ATE (ACVIM stage C HCM, group C) were enrolled (Table 1). Nearly 85% (70/83) of the cats were domestic shorthair (DSH) while a small number of cats belonged to domestic longhair (4), British shorthair (2), Russian Blue (2), Sphynx (2), Cornish Rex (1), Siamese (1) and Scottish Fold (1). No difference in mean body weight or age was observed between groups. Only five and six cats in group A had BP and echocardiography measurements, respectively. The means of LAD and LA. Ao were greater in groups B2 and C when compared with group B1, but no difference was found between groups B2 and C (Table 1).

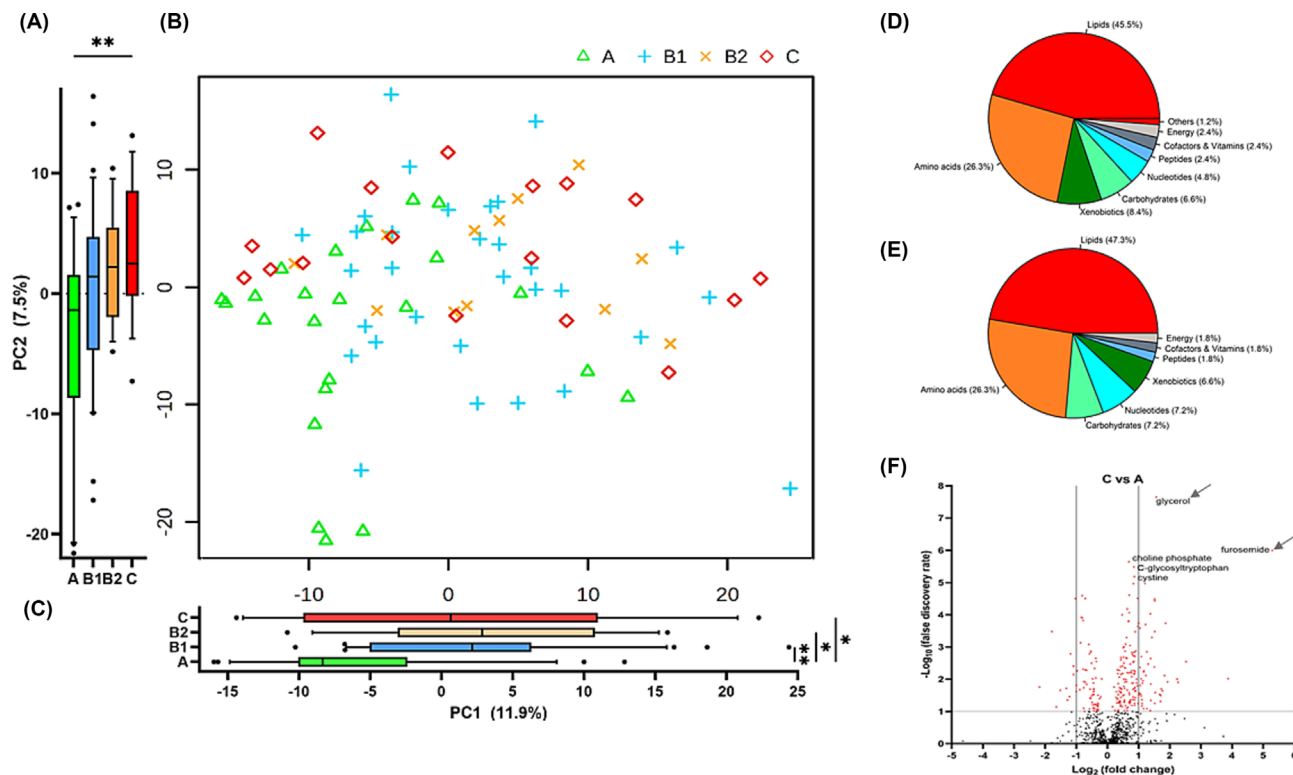
### Metabolomics

PCA revealed global shifts in metabolome among HCM and control groups (Figures 1A–C and S1). The first two PCs, PC1 and PC2, explained 11.9% and 7.5% of the data variance, respectively. On PC2, separations between groups C and A was evidenced (Figure 1A) while on PC1, all three HCM groups, B1, B2 and C, were well separated from group A, but had few discriminants among each other (Figure 1C). A total of 1253 metabolites were identified, of which 983 have known identities. Multiple linear regression analysis adjusted for sex, age and body weight identified 167 differential metabolites between control and HCM groups ( $FDR < 0.1$ , Table S1). The pathways with the greatest numbers of differential metabolites included lipids (45.5%), amino acids (26.3%), xenobiotics (8.4%), carbohydrates (6.6%) and nucleotides (4.8%) (Figure 1D). In group C, there was a preponderance of metabolites whose concentrations were increased rather than decreased compared with group A (Figure 1F). To the contrary, in group B2, there were more metabolites whose concentrations were decreased rather than increased compared with group A (Figure S2).

We compared the subset of data consisting of 70 DSH cats with the full dataset using the same statistical treatment. Despite the smaller sample size, data analysis on the DSH dataset resulted in 168 differential metabolites, of which 134/168 (79.8%) were shared between the two datasets (Table S2). In the pathway level, similar changes in metabolome were observed in the DSH dataset: the top five pathways were lipids (47.3%), amino acids (26.3%), carbohydrates (7.2%), nucleotides (7.2%) and xenobiotics (6.6%) (Figure 1E).

Blood glucose level was not different between groups. Serum concentration of glycerol was markedly increased in cats

**Figure 1** Global metabolome changes in cats with hypertrophic cardiomyopathy (HCM). (A–C) Principal component analysis (PCA) shows global metabolome change. (A,C) Boxplots show the differences of PC1 and PC2 among the four groups. The line in the middle of the box represents the median, and the whiskers are drawn to the 10th and 90th percentiles. The percentages of data variabilities explained by PC1 and PC2 are indicated. ANOVA and Tukey's multiple comparisons tests were used to compare the groups, and multiple testing error was adjusted. Asterisks indicate the adjusted *P* value: \**P* < 0.05; \*\**P* < 0.01. Pie charts show percentages of differential metabolites in each metabolic super pathways from (D) full dataset and (E) subset of data consisting of domestic shorthair cats. (F) Volcano plot shows the differences between groups C and A. The two vertical lines denote |fold change| = 2. Metabolites with false discovery rate (FDR) < 0.1 are coloured in red. The five most significant metabolites, including glycerol and cardiac drug furosemide (both with an arrow), are annotated.



with all three stages of HCM compared with control cats (Figures 1F and S2).

All cats were neutered. Sex and body weight were not statistically different among groups (*P* = 0.071, *P* = 0.065, respectively, Table 1). However, when cats from the three HCM groups were combined into a single group, the differences in sex and body weight between HCM and control groups were significant (*P* = 0.034, *P* = 0.003, respectively, Table S3). In addition, PCA analysis revealed that males accounted for more data variance on PC2, but not PC1, than females (Figure S3).

## Energy metabolism

### Free LCFAs and FAO intermediates

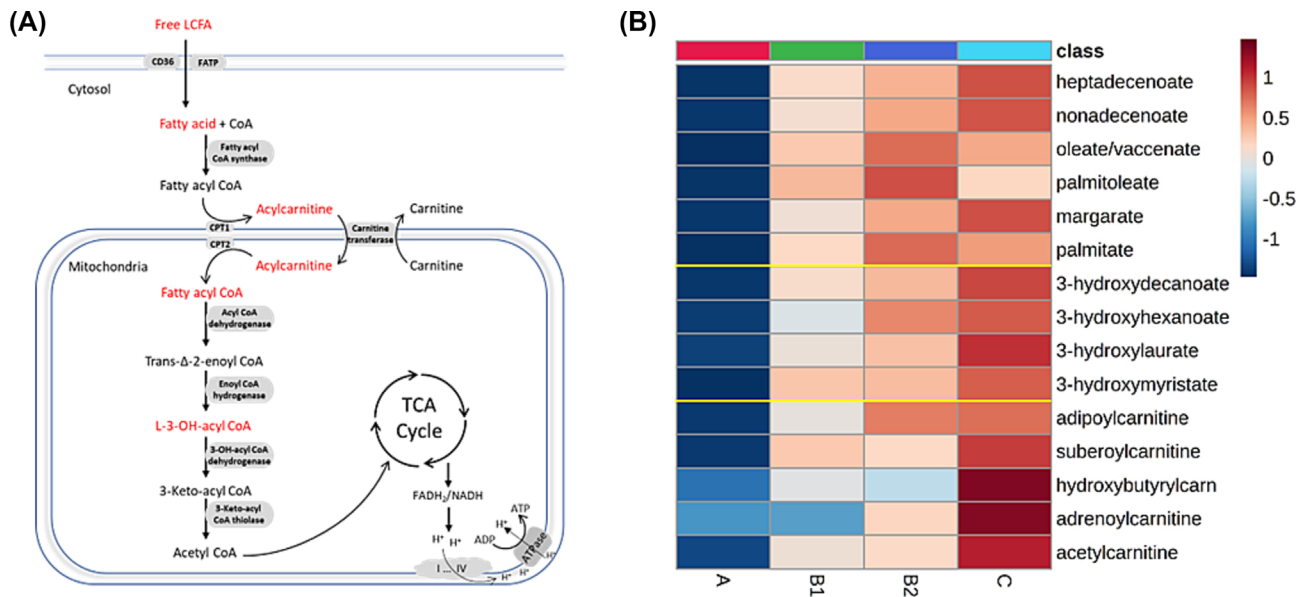
Free long-chain fatty acids (LCFAs) enter the cytosol and then cross the mitochondrial membrane for oxidation via FA transporters and the carnitine shuttle, respectively. Two carbons are cleaved during every cycle of FAO to generate acetyl-CoA, which enters the TCA cycle for oxidative phosphoryla-

tion (Figure 2A). Several saturated and unsaturated LCFAs, including four unsaturated oleate/vaccinate (C18:1), palmitoleate (C16:1n7), 10-heptadecenoate (C17:1n7) and 10-nonadecenoate (C19:1n9), and two saturated palmitate (C16:0) and margarate (C17:0), accumulated in the circulation in the HCM animals compared with healthy control animals (Figure 2B, top).

$\beta$ -Hydroxy FAs (also known as 3-hydroxy FAs), are formed by hydrating the double bond between the second and third carbons of *trans*-2-enoyl CoA (Figure 2A). Several of these, including 3-hydroxyhexanoate (C6), 3-hydroxydecanoate (C10), 3-hydroxylaurate (C12) and 3-hydroxymyristate (C14), accumulated in the circulation in cats with HCM groups versus control group (Figure 2B, middle). In addition,  $\alpha$ -hydroxybutyrate/ $\alpha$ -hydroxyisobutyrate, an  $\alpha$ -oxidation product by endoplasmic reticulum, accumulated in groups B1 and C compared with group A.

Acylcarnitines are formed from carnitine and acyl-CoA by carnitine acyltransferases in mitochondria or peroxisome (Figure 2A).<sup>45,46</sup> Serum concentrations of several fatty acyl-

**Figure 2** Fatty acid (FA) metabolism and oxidation. (A) Illustration of LCFA transport and  $\beta$ -oxidation in mitochondria. An LCFA undergoes four enzymatic reactions during  $\beta$ -oxidation in mitochondria leading to a shorter chain FA and an acetyl CoA, which enters the TCA cycle. (B) The heatmaps of LCFAs (top), 3-OH FAs (middle) and fatty acylcarnitines (bottom). From top, 10-heptadecenoate (C17:1n7), 10-nonadecenoate (C19:1n9), oleate/vaccenate (C18:1), palmitoleate (C16:1n7), dihomo-linolenate (C20:3n3 or n6), margarate (C17:0) and palmitate (16:0), 3-hydroxydecanoate (C10), 3-hydroxyhexanoate (C6), 3-hydroxylaurate (C12), 3-hydroxymyristate (C14), adipoylcarnitine (C6-DC), suberoylcarnitine (C8-DC), (S)-3-hydroxybutyrylcarnitine, adrenoylcarnitine (C22:4) and acetylcarnitine (C2).



carnitines, most of which were short- or medium-chained (C2–C8), were increased in stages B1, B2 and C when compared with animals in group A (Figure 2C, bottom).

#### TCA cycle intermediates and creatine phosphate shuttle

Several TCA cycle intermediates, including aconitate, succinate and alpha-ketoglutarate, accumulated in the serum in cats with preclinical (B1 and B2) and clinical (C) HCM compared with the control animals (Figure 3B–D). The concentration of creatine phosphate (PCr), which carries and transfers high energy phosphate to cardiac myofibrils, was increased by more than 1.5-fold in groups C and B1 compared with A (Figure 3E). The level of inorganic phosphate, a substrate of ATP synthesis, was also increased in group C versus group B2 (Figure 3F), but the difference between groups C and B1 was not significant (adjusted  $P = 0.091$ ).

#### NAD<sup>+</sup> biosynthesis

Nicotinamide adenine dinucleotide or NAD<sup>+</sup> is an important coenzyme central to bioenergetics and redox homeostasis. There are three main NAD<sup>+</sup> pathways, the main salvage pathway from nicotinamide and nicotinamide riboside, the de novo synthesis pathway from Tryptophan, and the Preiss–Handler pathway from nicotinic acid (Figure 3A). The concentration of nicotinamide, precursor for the major NAD<sup>+</sup> salvage pathway, decreased twofold in groups B1 and B2 compared with group A (Figure 3G). Tryptophan, the precursor for the de novo NAD<sup>+</sup> biosynthesis pathway was reduced in

group C compared with group A (Figure 3H). In mammals, a small percentage (<5%) of tryptophan is also used for the biosynthesis of serotonin, which was previously shown to be associated with the severity of naturally occurring mitral valve disease in dogs.<sup>47</sup> The concentration of serotonin was reduced in C versus B1 (adjusted  $P = 0.027$ ) (Figure 3I).

#### Phospholipids and sphingolipids

Cardiac sarcolemma is a dynamic fluid bilayer that constitutes a variety of lipid species to provide stability, fluidity and permeability of the membranes.<sup>48</sup> The majority of lipids in the membranes are glycerophospholipids (GPLs), sphingolipids (SLs) and cholesterol.

#### GPLs

The GPLs comprise about 80% of the total lipids in the membranes of all cell types. GPL consists of a polar head group, such as choline, ethanolamine, inositol or serine, and two fatty acyl chains attached to a glycerol backbone.<sup>49</sup> Serum concentrations of many species of glycerophosphatidylcholine (GPC), glycerophosphatidylethanolamine (GPE) and glycerophosphatidylinositol (GPI) were reduced in cats with HCM compared with the control (Figure 4A). These changes were evident as early as preclinical B2 stage and became more pronounced in stage B2. However, little difference was observed between stage C and stage B1 or B2.

**Figure 3** Energy metabolism. (A) Nicotinamide adenine dinucleotide (NAD<sup>+</sup>) biosynthesis pathways: the main salvage pathway from nicotinamide (NAM) and nicotinamide riboside (NR) via nicotinamide mononucleotide (NMN), the de novo pathway from tryptophan (TRP) via quinolinic acid (QA); and the Preiss–Handler pathway from nicotinic acid (NA). TCA cycle intermediates, (B–D) succinate, aconitate, and  $\alpha$ -ketoglutarate, (E,F) creatine phosphate and inorganic phosphate, (G) nicotinamide, (H) tryptophan and (I) serotonin (5-HT). For phosphate (F), the adjusted *P* value between groups B1 and C was 0.091. The line in the box indicates the median, and the whiskers indicate 10th and 90th percentiles. Asterisks denote adjusted *P* values from Tukey’s multiple comparisons test: \**P* < 0.05, \*\**P* < 0.01. Negative values are the results of data transformation using the natural log on data between (0, 1). AU, arbitrary unit. All metabolites were significant for the linear model [false discovery rate (FDR) < 0.1].

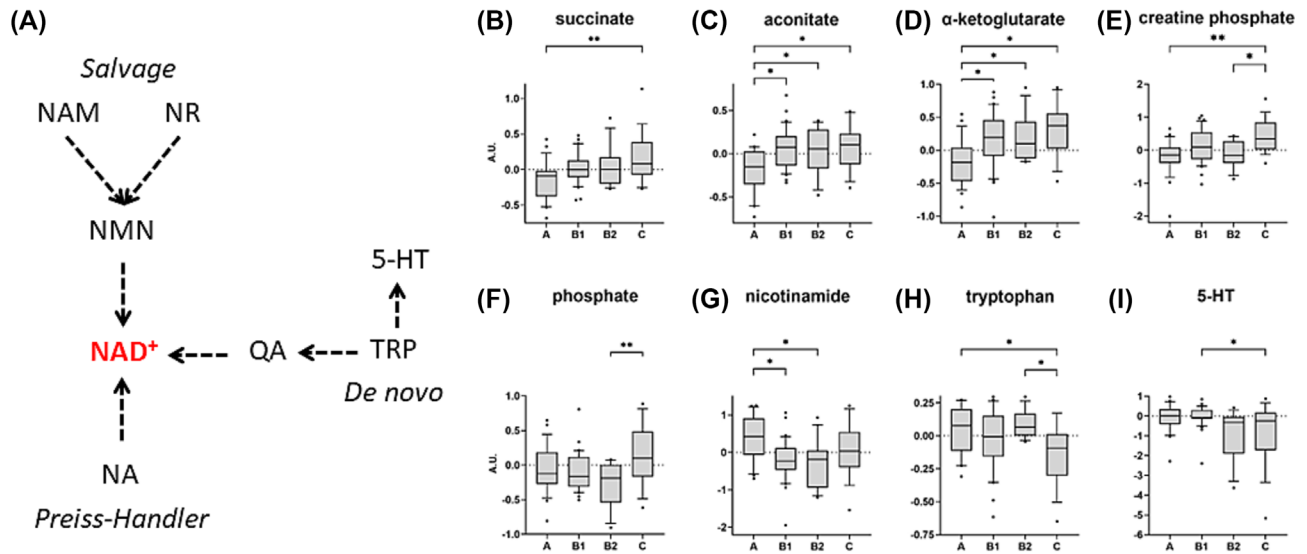
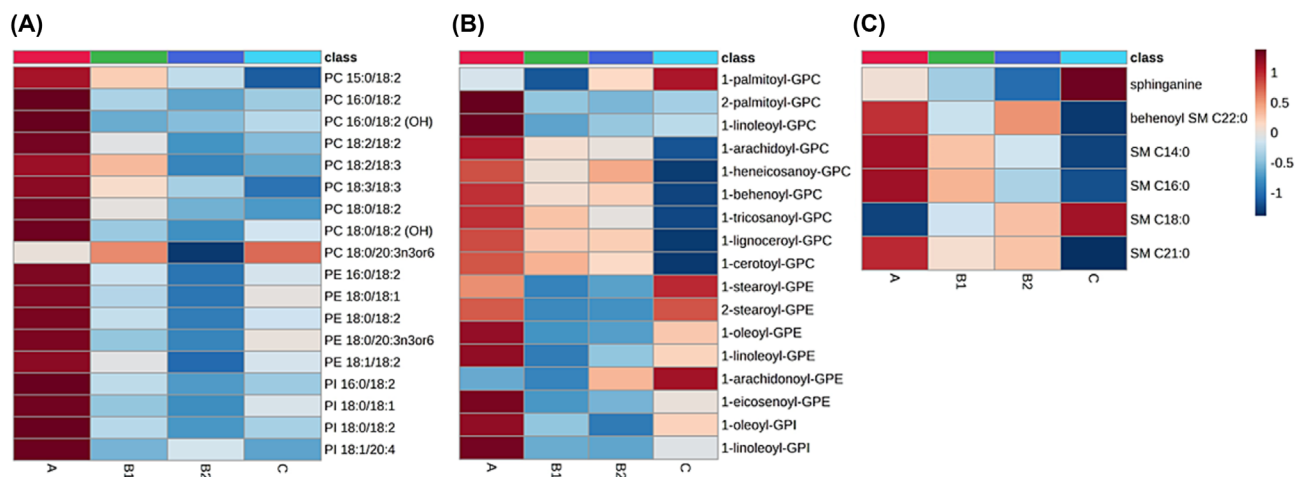


**Figure 4** Lipid metabolism. (A) Glycerophospholipids with different polar head groups, GPL-choline (PC, top), GPL-ethanolamine (PE, middle) and GPL-inositol (PI, bottom). (B) Lysophospholipids: LPL-choline (GPC, top), LPL-ethanolamine (GPE, middle) and LPL-inositol (GPI, bottom). (C) Spingomyelins (SMs) are the main sphingolipids in the membranes.



### Lysophospholipids

The lysophospholipids (LPLs) are a special group of GPLs with one fatty acyl chain attached a glycerol backbone.<sup>49</sup> They are found in small amounts in the biological membranes. The levels of lysophosphatidylcholines were decreased in groups

B1 and B2 compared with A. The changes became more pronounced in group C (Figure 4B, GPCs). For lysophosphatidylethanolamines and lysophosphatidylinositols, to the contrary, the decreases were observed in groups B1 and B2 but not in group C (Figure 4B, GPEs and GPIs).

### Sphingomyelins

Unlike GPLs, SLs contain a sphingosine backbone instead of a glycerol backbone.<sup>49</sup> More than 85% of SLs are sphingomyelins (SMs), which comprise 4%–18% of all sarcolemmal membrane lipids.<sup>48,50</sup> Serum concentrations of several SM species were decreased in group C compared with A (Figure 4C). In contrast, the serum levels of both SM C18:0 and sphinganine, the precursor of sphingosine and ceramide, were increased in group C.

## Glutathione pathways

### Glutathione synthesis

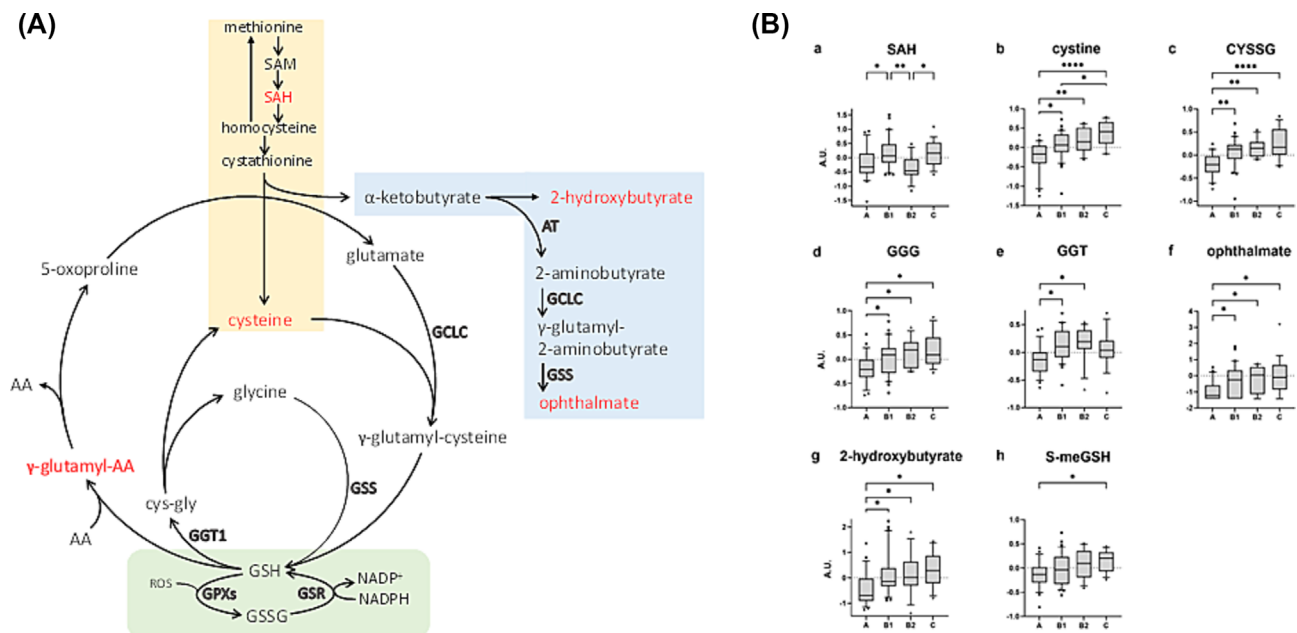
Glutathione (GSH) plays a key role in mitochondrial redox balance.<sup>18</sup> Several intermediates of the GSH pathways accumulate in HCM cats (Figure 5A). The concentration of S-adenosylhomocysteine (SAH) was increased in group B1 compared with group A, but was decreased in group B2 compared with group B1 or C (Figure 5B,a). The concentrations of cystine, the predominant, oxidized disulfide form of cysteine in the blood, were higher in HCM stages B1, B2 and C compared with controls (Figure 5B,b), suggesting a

pro-oxidative status in the HCM state (Figure 5B,b). Similar change was observed in cysteine-glutathione disulfide (CYSSG, Figure 5B,c), which is formed upon oxidative stress and GSH depletion. The levels of two  $\gamma$ -glutamyl-amino acids,  $\gamma$ -glutamyl-glutamate and  $\gamma$ -glutamyl-tryptophan, were elevated in HCM groups compared with control group (Figure 5B,d,e).

### Ophthalmate synthesis

Ophthalmate (OPH), an endogenous analog of GSH where the cysteine moiety is replaced by  $\alpha$ -aminobutyrate (Figure 5A, blue area).<sup>51–54</sup> The serum concentration of OPH was increased by more than two-fold in groups B1 and B2 and four-fold in group C when compared with group A (Figure 5B,f). The concentration of  $\alpha$ -hydroxybutyrate (or  $\alpha$ -hydroxyisobutyrate), the product of  $\alpha$ -ketobutyrate by  $\alpha$ -hydroxybutyrate dehydrogenase, was also increased by about two-fold in groups B1, B2 and C versus group A (Figure 5B,g).<sup>55</sup> S-methylglutathione (S-meGSH), another GSH analog with methylated SH group of the cysteine moiety, was increased in groups B2 and C compared with group A (Figure 5B,h).

**Figure 5** The glutathione and ophthalmate pathways. (A) Methionine undergoes transmethylation and transsulfuration (yellow) reactions to produce cysteine (yellow). Cysteine then conjugates with glutamate to form the  $\gamma$ -glutamyl-cysteine dipeptide by glutamate-cysteine ligase (GCLC). The glutathione synthase (GSS) catalyses the addition of glycine to the dipeptide to form glutathione (GSH). Ophthalmate (OPH) synthesis pathway (blue) shares the same enzymes of GSH biosynthesis. Metabolites that were altered in the study were highlighted in red. (B) The changes of serum metabolites in GSH and OPH pathways. AT, amidinotransferase; CYSSG, cysteine-glutathione disulfide; GGG,  $\gamma$ -glutamyl-glutamate; GGT,  $\gamma$ -glutamyl-tryptophan; SAH, S-adenosylhomocysteine; S-meGSH, S-methylglutathione. The line in the box indicates the median, and the whiskers indicate 10th and 90th percentiles. Asterisks denote adjusted *P* values from Tukey's multiple comparisons test: \**P* < 0.05, \*\**P* < 0.01, \*\*\**P* < 0.001, \*\*\*\**P* < 0.0001. Negative values are the results of data transformation using the natural log on data between (0, 1). AU, arbitrary unit. All metabolites were significant for the linear model [false discovery rate (FDR) < 0.1].



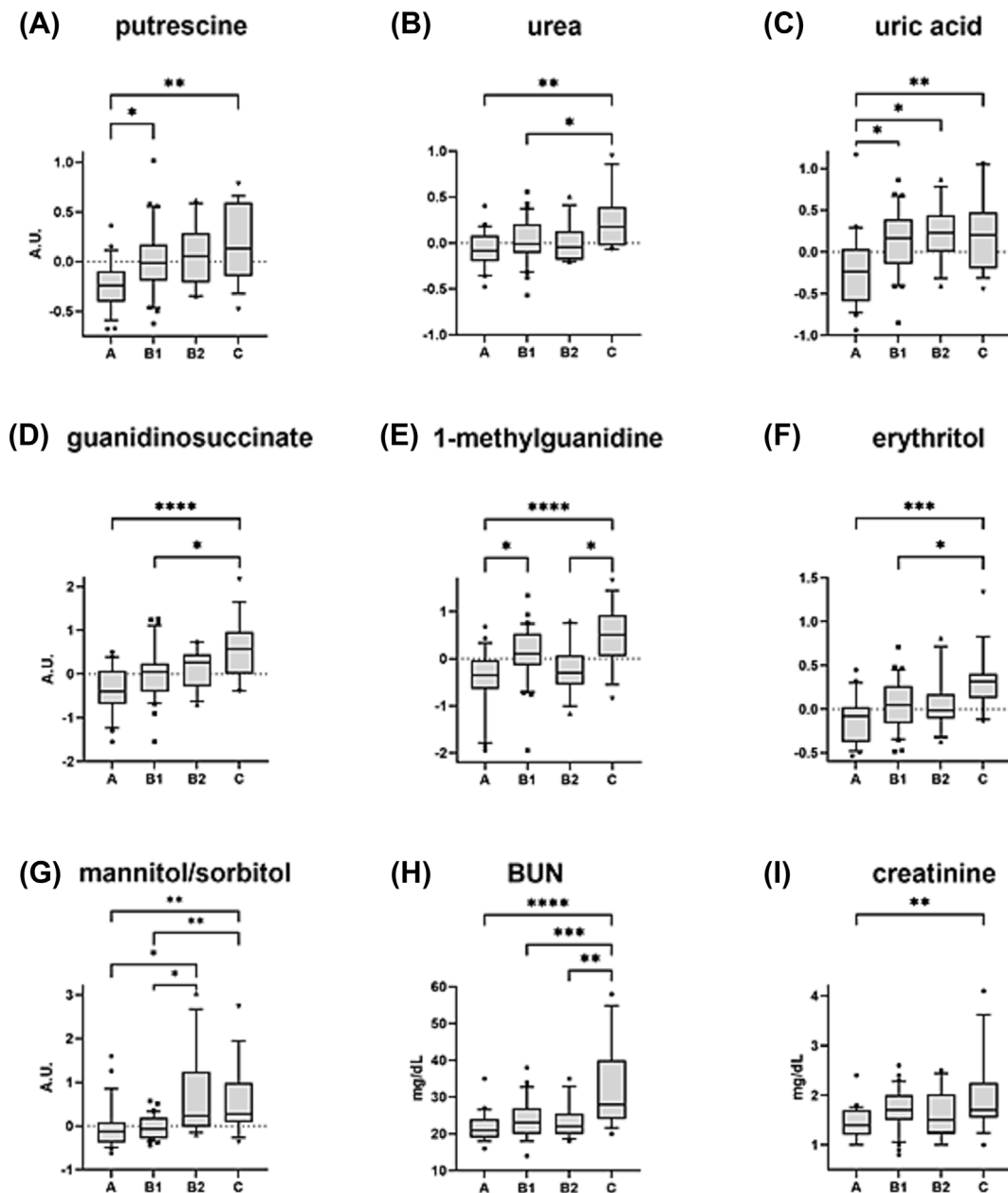


## Renal excretion of drugs and uremic toxins

Urinary excretion of uremic toxins and many exogenous small molecules (including drugs) is handled by organic anionic transporters in the proximal tubules of the kidneys. Serum

concentrations of several uremic toxins, including guanidino compounds guanidinosuccinate and 1-methylguanidine, and protein bound polyamine putrescine, were increased in HCM cats (*Figure 6A–G*, Table S4). Putrescine was different in groups B1 and C compared with group A (adjusted

**Figure 6** Uremic toxins and nitrogenous products. (A–I) Putrescine, urea, uric acid, guanidinosuccinate, 1-methylguanidine, erythritol, and mannitol/sorbitol, blood urea nitrogen (BUN) and creatinine. (A–G) Data were transformed using natural logarithm and auto-scaled and expressed using arbitrary unit (AU) and shown in mean and SEM. Negative values were the results of data transformation using the natural log on small numbers between (0, 1). (H,I) Concentrations of BUN and creatinine in mg/dL. The line in the box indicates the median, and the whiskers indicate 10th and 90th percentiles. Asterisks denote adjusted *P* values from Tukey's multiple comparisons test: \**P* < 0.05, \*\**P* < 0.01, \*\*\**P* < 0.001, \*\*\*\**P* < 0.0001. All metabolites were significant in the linear model [false discovery rate (FDR) < 0.1].



$P < 0.05$ ), but not between group B2 and group A (adjusted  $P = 0.101$ ). While urea was higher in group C only, uric acid (urate), a metabolite from purine metabolism, was increased in all groups of HCM cats compared with control cats. In addition, furosemide, a medication to treat oedema caused by CHF, was increased by 40-fold in group C versus group A (Figure 1F), and atenolol for high blood pressure accumulated in circulation in B2, but not C, compared with A (Figure S2b).

Blood urea nitrogen (BUN) was elevated in group C compared with groups A, B1 and B2, and serum creatinine level was also higher in group C compared with group A (Figure 6I,J).

## Steroid hormones

Cortisol is an active form of glucocorticoid hormone cortisone while 11-dehydrocorticosterone is the inactive form of corticosterone.<sup>56</sup> The concentrations of cortisol and 11-dehydrocorticosterone were increased all three groups (B1, B2 and C) compared with the control group (Figure S4).

## Discussion

One of the main advantages of our study is the uniform genetic background of the majority of DSH cats enrolled. This uniformity reduced variability, enhancing our ability to detect changes that would otherwise not be possible in a heterogeneous background. A comparison between the full dataset and the subset of data consisting of only DSH cats showed similar changes in the pathway level, suggesting that genetic background had a relative small contribution to the reported changes.

Cardiac metabolism exhibits distinctive substrate utilization, oxidative phosphorylation and distinctive cellular organization to enable transfer of ATP from mitochondria to cardiac myofibrils.<sup>12,57</sup> The main energy substrates for the normal heart are LCFAs. Inside the mitochondria, each LCFA undergoes several rounds of FA  $\beta$ -oxidation (FAO) to generate acetyl-CoA (Figure 2A). Human FAO disorders are a group of rare, autosomal recessive mutations in the genes that encode the enzymes and proteins involved in FA transports and oxidation.<sup>58–60</sup> These disorders are characterized by an accumulation of FAs, 3-hydroxy FAs (3-OH FAs) and fatty acylcarnitines in the circulation.<sup>61,62</sup> Circulating acylcarnitines accumulate as a result of incomplete or inefficient FAO and have been used as diagnostic markers for disorders in peroxisomal or mitochondrial oxidation processes.<sup>63–65</sup> The failing heart increases its reliance on ketones for fuel in the context of reduced capacity for FAO.<sup>20,66</sup> Lommi et al. reported augmentations of circulating free FAs and ketones in people with CHF versus healthy controls.<sup>67–69</sup> Increased myocardial expressions of genes and proteins implicated in the FAO and ke-

tone oxidation pathways were observed while reductions of myocardial concentrations of ketones, FAO and TCA cycle intermediates were reported in human HF patients compared with controls.<sup>20,22,29,32,70</sup> The findings from our study and others suggested reductions of myocardial FAO and oxidative phosphorylation in cats with HCM compared with control cats. This hypothesis should be tested using cardiac tissue samples in the future.

Several TCA cycle intermediates such as succinate, aconitate and  $\alpha$ -ketoglutarate accumulated in the serum of cats with preclinical and clinical HCM, suggesting abnormal flux through mitochondrial oxidative phosphorylation and ATP production. The accumulation of circulating PCr, a storage for high-energy phosphates in myocardium,<sup>71</sup> signifies impaired energy transfer from mitochondria to cardiac myofibrils. In dogs with mitral valve disease, serum concentrations of creatine were increased compared with healthy controls.<sup>72</sup> In humans, myocardial levels of creatine and total PCr were reduced by 35% and 55% in patients with CHF compared with control individuals, respectively.<sup>70</sup> A recent report showed an even more substantial reduction of myocardial PCr by more than 90% in human HCM hearts compared with control hearts.<sup>29</sup> This change was interpreted as an adaptive response to maintain ATP/ADP (adenosine diphosphate) ratio through ATP synthesis by creatine kinase reaction in the context of diminished ATP production in the failing hearts.<sup>73</sup> Increased levels of circulating creatine and PCr may suggest impaired creatine uptake from blood to myocardium and some uncoupling of energy production and transfer. Inorganic phosphate is the substrate for ATP synthase. Its accumulation could also indicate perturbed oxidative phosphorylation and ATP synthesis.

In mammalian cells, NAD<sup>+</sup> is an essential cofactor for numerous enzymes involved in mitochondrial bioenergetics and redox homeostasis. There are three classical pathways for NAD<sup>+</sup> biosynthesis, the main salvage pathway that recycles NAM or nicotinamide riboside, the de novo pathway from amino acid L-tryptophan and the Preiss–Handler pathway from nicotinic acid or niacin.<sup>74</sup> The concentration of NAM was significantly reduced in the preclinical groups B1 and B2 by two-fold compared with the control group A, suggesting reduced bioavailability of NAM. The tryptophan level was also reduced in the clinical group C compared with group B2 or A. Because the salvage pathway accounts for a majority of NAD<sup>+</sup> synthesis, a depletion of nicotinamide in the blood could have a profound impact on myocardial NAD<sup>+</sup> supply. Previs et al. reported that myocardial NAM and NMN, precursors for NAD<sup>+</sup>, were more abundant in human HCM heart compared with control hearts, possibly due to reduced myocardial availability of ATP required for NAD<sup>+</sup> synthesis.<sup>29</sup> Recently, trigonelline supplementation to boost NAD<sup>+</sup> level showed promise to reduce age-associated muscle decline in a preclinical rodent study,<sup>75</sup> the strategy that could provide a path to improve NAD<sup>+</sup> bioavailability for HCM patients.

Mitochondria are the primary intracellular site for oxygen consumption. Due to its high energy demand, the heart has the greatest mitochondrial abundance among all organs.<sup>9,76</sup> Mitochondrial consumption of molecular oxygen in the respiratory chain drives ATP synthesis, but also generates large amounts of ROS, which in excess can lead to mitochondrial dysfunction, apoptosis and broader signalling abnormalities. Mitochondria are equipped with a range of antioxidant defence systems, among which GSH is the critical component, preventing and repairing oxidative damage.<sup>24,77</sup> Serum concentrations of several intermediates of the GSH synthesis pathway, including  $\gamma$ -glutamyl-amino acids, SAH and cystine were increased in HCM cats (Figure 5A). OPH, a GSH analog lacking the thiol group, was widely presumed to be an accidental by-product of GSH biosynthesis of the same enzymes. The postulation that the OPH is synthesized when GSH is depleted and when the hepatic availability of cysteine is limited seems to be an oversimplification.<sup>51–54,78</sup> However, emerging evidence has demonstrated that OPH plays a modulatory role in GSH bioavailability and utilization, possibly through competitive inhibition of GSH transport and utilization, and to disrupt or mimic the effects of GSH.<sup>78</sup> It is remarkable that the serum level of OPH increased two-fold in group B1 cats and up to four-fold in group C cats, compared with control cats. A targeted study to quantify OPH using a different cohort of cats would help establish the link of OPH as a redox indicator and biomarker in cats with HCM. A wealth of experimental work has demonstrated a link between reduced GSH level and the pathogenesis and progression of many human diseases, including cardiovascular disease.<sup>79,80</sup> Elevated myocardial GSSG/GSH ratio and cystine, which is the oxidized disulfide form of cysteine, and reduced level of glutathione peroxidase were reported in human HCM heart samples compared with the control samples.<sup>32</sup> In dogs with preclinical MMVD, the serum concentration of GSSG was increased while dogs with CHF had a lower GSH/GSSG ratio compared with healthy dogs.<sup>26,27</sup> Taken together, available evidence from both human and animal studies has demonstrated that the redox homeostasis is disrupted and myocardial capacity to neutralize ROS is impaired in the HCM hearts.

Retention of uremic solutes contributes to the uremic syndromes, which are associated with oxidative stress, inflammation, fibrosis and cellular toxicity.<sup>81,82</sup> How uremic toxins are metabolized and handled in the kidneys is not fully understood. Emerging evidence suggests both glomerular filtration and active tubular transport are involved. Cats with stage C HCM had increased levels of BUN and creatinine, suggesting reduced renal filtration and function. Consistently, cats with HCM had elevated levels of circulating uremic toxins, including putrescine, urea, uric acid, guanidinosuccinate and 1-methylguanidine. In human dialysis patients, guanidinosuccinate and methylguanidine accumulate to 100–200 times normal levels, compared with 1–20 times normal levels of creatinine<sup>83</sup> and were assigned the

highest indexes for uremic toxicity by the European Uremic Toxin Work Group.<sup>82</sup> Putrescine, a protein-bound polyamine, which cannot be removed by passive filtration in the glomeruli, is eliminated by the concerted effort of several transporters in the proximal tubules. Retention of these uremic solutes further exacerbates injuries to cardiomyocytes through activation of pathways for oxidative stress, chronic inflammation and fibrosis. Our findings suggested the intricate interplay between uremic toxins, renal function and myocardial disease in cats although these features may also reflect other factors including renal perfusion.

More than 45% of the differential metabolites belonged to lipid metabolism pathways, suggesting aberrant lipid metabolism in cats with HCM. The majority of these lipids were GPLs with two fatty acyl chains attached to a glycerol backbone. LPLs, with one fatty acyl chain removed from GPLs, constitute only a small amount of the membrane lipids. SLs differ from GPLs and LPLs in that SLs have a sphingosine backbone in place of glycerol.<sup>48,49</sup> Our analysis demonstrated that serum levels of the majority of GPL, LPL and SL species were reduced in HCM cats compared with control cats. To the contrary, there were a few lipid species whose levels were increased (e.g., 1-palmitoyl-GPC, 1-arachidonoyl-GPE, sphinganine and SM C18:0) or returned to the normal level (e.g., 1-stearoyl-GPE and 2-stearoyl-GPE). Perturbations of cardiac sarcolemmal lipids lead to structural and functional changes in cardiac myocytes.<sup>84</sup> Changes in lipid profile are associated with sarcolemmal membrane perturbations in human and animal models of cardiomyopathy.<sup>50,85,86</sup> LPLs play both structural and functional roles. For example, LPLs are known to act as signalling mediators via G protein-coupled receptors and are associated with cardiovascular disease, cardiac myocyte hypertrophy and cardioprotection against ischaemia/reperfusion.<sup>85,87</sup> SMs also act as a reservoir of lipid signalling molecules for a wide array of biological processes.<sup>88,89</sup> Altered concentrations of several SMs have been documented in atherosclerosis, cardiomyopathies and valvular disease in humans.<sup>89</sup> Our study provides evidence of impaired lipid metabolism and signalling in feline HCM, but the mechanisms of these changes and their potential contributions to the development and progression of HCM in cats will require further studies.

There are some limitations in our study. Diet, which is a potential confounding factor on the serum metabolome, was not controlled in this study, and fasting was not required for blood draws. Our HCM cohorts included 14 females versus 46 males compared with the sex-balanced control group. Statistical analysis showed sex and body weight were not significantly different among the four groups. However, when all HCM cats were combined into a single group and compared with the control cats, sex and body weight were no longer independent of HCM status. Multiple studies have demonstrated that HCM occurs more frequently in males than females in both humans<sup>90,91</sup> and cats.<sup>92–94</sup> In feline HCM, the

odds ratio for males was 7.9 versus females, after adjusting for age and body weight,<sup>92</sup> and DSH was the most common breed.<sup>93</sup> A greater effort should be made to enrol more female subjects in the future studies. Despite efforts to exclude potential comorbidities, it is possible that undiscovered disease might be present in the studied cats. In spite of these limitations, our data demonstrated that cats with HCM have (1) reduced capacity for FAO, with inefficient oxidative phosphorylation and elevated ROS production, (2) impaired glutathione homeostasis and redox balance as evidenced by the elevated level of OPH in the circulation of HCM cats, (3) aberrant lipid metabolism and reprogramming, and (4) reduced renal function and capacity to eliminate nitrogenous wastes, some drugs and uremic toxins. Our study sheds light on the pathophysiology of feline HCM and paves the way for future systems biology studies of the mechanisms of hypertrophy. Ultimately, we hope that learnings from cats could be applied to improve heart health in both cats and humans.

## Acknowledgements

We thank Dr. Yeonji Cho for data assistance, Heather Brown for laboratory assistance and Dr. Philipp Gut for critical reading of the manuscript.

## Conflict of interest

None declared.

## Conflict of interest statement

Q. L., B. V. B. and P. S. are current employees of Nestlé Purina PetCare Company.

## References

1. Ferasin L, Sturgess CP, Cannon MJ, Caney SMA, Gruffydd-Jones TJ, Wotton PR. Feline idiopathic cardiomyopathy: a retrospective study of 106 cats (1994–2001). *J Feline Med Surg* 2003;**5**: 151–159. doi:10.1016/S1098-612X(02)00133-X
2. Payne JR, Brodbelt DC, Luis FV. Cardiomyopathy prevalence in 780 apparently healthy cats in rehoming centres (the CatScan study). *J Vet Cardiol* 2015;**17**: S244–S257. doi:10.1016/j.jvc.2015.03.008
3. Paige CF, Abbott JA, Elvinger F, Pyle RL. Prevalence of cardiomyopathy in apparently healthy cats. *J Am Vet Med Assoc* 2009;**234**:1398–1403. doi:10.2460/javma.234.11.1398
4. Fox PR. Hypertrophic cardiomyopathy. Clinical and pathologic correlates. *J Vet Cardiol* 2003;**5**:39–45. doi:10.1016/S1760-2734(06)70051-0
5. Luis Fuentes V, Abbott J, Chetboul V, Côté E, Fox PR, Häggström J, et al. ACVIM consensus statement guidelines for the classification, diagnosis, and management of cardiomyopathies in cats. *J Vet Intern Med* 2020;**34**: 1062–1077. doi:10.1111/jvim.15745
6. Fox PR, Keene BW, Lamb K, Schober KA, Chetboul V, Luis Fuentes V, et al. International collaborative study to assess cardiovascular risk and evaluate long-term health in cats with preclinical hypertrophic cardiomyopathy and apparently healthy cats: the REVEAL study. *J Vet Intern Med* 2018;**32**: 930–943. doi:10.1111/jvim.15122
7. O'Donnell K, Adin D, Atkins CE, DeFrancesco T, Keene BW, Tou S, et al. Absence of known feline MYH7 and MYBPC3 variants in a diverse cohort of cats with hypertrophic cardiomyopathy. *Anim Genet* 2021;**52**:542–544. doi:10.1111/age.13074
8. Boeykens F, Abitbol M, Anderson H, Dargar T, Ferrari P, Fox PR, et al. Classification of feline hypertrophic

## Supporting information

Additional supporting information may be found online in the Supporting Information section at the end of the article.

**Data S1.** Supporting Information.

**Figure S1.** PCA plots show global metabolome changes among the four groups of cats with and without HCM. Only the first three PCs are shown.

**Figure S2.** Volcano plots show the differences between (a) B1 vs A and (b) B2 vs A. The two vertical lines denote |fold change| = 2. Metabolites with FDR < 0.1 are coloured in red. Glycerol and atenolol are pointed by an arrow.

**Figure S3.** Principal component analysis (PCA) shows global metabolome change. (a,c) Boxplots compare the differences of PC1 and PC2 between males and females. The line in the middle of the box represents the median, and the whiskers are drawn to the 10<sup>th</sup> and 90<sup>th</sup> percentiles. The percentages of data variabilities explained by PC1 and PC2 are indicated. Student's t test was used to compare F and M groups. Asterisks indicate the adjusted *P* value: \*\* < 0.01.

**Figure S4.** Serum concentrations of cortisol and 11-dehydrocorticosterone. Data were transformed using natural logarithm and auto-scaled, and expressed using arbitrary unit (AU). Data are shown in mean and SEM. Negative values were the results of data transformation using the natural log on small numbers between (0, 1). Asterisks denote adjusted *P* values from Tukey's multiple comparisons test: \* < 0.05, \*\* < 0.01, \*\*\* < 0.001, \*\*\*\* < 0.0001.

**Table S1.** Supporting Information.

**Table S2.** Supporting Information.

**Table S3.** Sex and body weight between control and HCM cats.

**Table S4.** Serum uremic toxin concentrations in healthy and HCM cats.

- cardiomyopathy-associated gene variants according to the American College of Medical Genetics and Genomics guidelines. *Front Vet Sci* 2024; **11**:1327081. doi:10.3389/fvets.2024.1327081
9. Pagliarini DJ, Calvo SE, Chang B, Sheth SA, Vafai SB, Ong SE, *et al.* A mitochondrial protein compendium elucidates complex I disease biology. *Cell* 2008; **134**:112-123. doi:10.1016/j.cell.2008.06.016
  10. Wang Z, Ying Z, Bosty-Westphal A, Zhang J, Schautz B, Later W, *et al.* Specific metabolic rates of major organs and tissues across adulthood: evaluation by mechanistic model of resting energy expenditure. *Am J Clin Nutr* 2010; **92**:1369-1377. doi:10.3945/ajcn.2010.29885
  11. Feruglio FS, Migheli B, Campus S, Pandolfo G. Studies on the circulation of an organ: simultaneous determination of coronary, cerebral and renal blood flow, of cardiac output and of the oxygen consumption of the heart, brain and kidneys. *Boll Soc Ital Biol Sper* 1960; **36**:952-954. PMID: 13699201.
  12. Neubauer S. The failing heart—an engine out of fuel. *N Engl J Med* 2007; **356**:1140-1151. doi:10.1056/NEJMra063052
  13. van der Vusse GJ, van Bilsen M, Glatz JF. Cardiac fatty acid uptake and transport in health and disease. *Cardiovasc Res* 2000; **45**:279-293. doi:10.1016/s0008-6363(99)00263-1
  14. Lopaschuk GD, Ussher JR. Evolving concepts of myocardial energy metabolism: more than just fats and carbohydrates. *Circ Res* 2016; **119**:1173-1176. doi:10.1161/CIRCRESAHA.116.310078
  15. Lopaschuk GD, Belke DD, Gamble J, Itoi T, Schonekess BO. Regulation of fatty acid oxidation in the mammalian heart in health and disease. *Biochim Biophys Acta* 1994; **1213**:263-276. doi:10.1016/0005-2760(94)00082-4
  16. Lopaschuk GD, Ussher JR, Folmes CD, Jaswal JS, Stanley WC. Myocardial fatty acid metabolism in health and disease. *Physiol Rev* 2010; **90**:207-258. doi:10.1152/physrev.00015.2009
  17. Balaban RS, Nemoto S, Finkel T. Mitochondria, oxidants, and aging. *Cell* 2005; **120**:483-495. doi:10.1016/j.cell.2005.02.001
  18. Mailloux RJ, McBride SL, Harper ME. Unearthing the secrets of mitochondrial ROS and glutathione in bioenergetics. *Trends Biochem Sci* 2013; **38**:592-602. doi:10.1016/j.tibs.2013.09.001
  19. Aubert G, Martin OJ, Horton JL, Lai L, Vega RB, Leone TC, *et al.* The failing heart relies on ketone bodies as a fuel. *Circulation* 2016; **133**:698-705. doi:10.1161/CIRCULATIONAHA.115.017355
  20. Horton JL, Davidson MT, Kurishima C, Vega RB, Powers JC, Matsuura TR, *et al.* The failing heart utilizes 3-hydroxybutyrate as a metabolic stress defense. *JCI Insight* 2019; **4**:e124079. doi:10.1172/jci.insight.124079
  21. Selvaraj S, Kelly DP, Margulies KB. Implications of altered ketone metabolism and therapeutic ketosis in heart failure. *Circulation* 2020; **141**:1800-1812. doi:10.1161/CIRCULATIONAHA.119.045033
  22. Bedi KC Jr, Snyder NW, Brandimarto J, Aziz M, Mesaros C, Worth AJ, *et al.* Evidence for intramyocardial disruption of lipid metabolism and increased myocardial ketone utilization in advanced human heart failure. *Circulation* 2016; **133**:706-716. doi:10.1161/CIRCULATIONAHA.115.017545
  23. Circu ML, Aw TY. Reactive oxygen species, cellular redox systems, and apoptosis. *Free Radic Biol Med* 2010; **48**:749-762. doi:10.1016/j.freeradbiomed.2009.12.022
  24. Chai YC, Miesel JJ. Glutathione and glutaredoxin-key players in cellular redox homeostasis and signaling. *Antioxid (Basel)* 2023; **12**:12. doi:10.3390/antiox12081553
  25. Christiansen LB, Dela F, Koch J, Hansen CN, Leifsson PS, Yokota T. Impaired cardiac mitochondrial oxidative phosphorylation and enhanced mitochondrial oxidative stress in feline hypertrophic cardiomyopathy. *Am J Physiol Heart Circ Physiol* 2015; **308**:H1237-H1247. doi:10.1152/ajpheart.00727.2014
  26. Freeman LM, Rush JE, Milbrun PE, Blumberg JB. Antioxidant status and biomarkers of oxidative stress in dogs with congestive heart failure. *J Vet Intern Med* 2005; **19**:537-541. doi:10.1892/0891-6640(2005)19[537:asaboo]2.0.co;2
  27. Li Q, Freeman LM, Rush JE, Huggins GS, Kennedy AD, Labuda JA, *et al.* Veterinary medicine and multi-omics research for future nutrition targets: metabolomics and transcriptomics of the common degenerative mitral valve disease in dogs. *OMICS* 2015; **19**:461-470. doi:10.1089/omi.2015.0057
  28. Lozhkin A, Vendrov AE, Ramos-Mondragón R, Canugovi C, Stevenson MD, Herron TJ, *et al.* Mitochondrial oxidative stress contributes to diastolic dysfunction through impaired mitochondrial dynamics. *Redox Biol* 2022; **57**:102474. doi:10.1016/j.redox.2022.102474
  29. Previs MJ, O'Leary TS, Morley MP, Palmer BM, LeWinter M, Yob JM, *et al.* Defects in the proteome and metabolome in human hypertrophic cardiomyopathy. *Circ Heart Fail* 2022; **15**:e009521. doi:10.1161/CIRCHEARTFAILURE.121.009521
  30. Jansen M, Schuldt M, van Driel BO, Schmidt AF, Christiaans I, van der Crabben SN, *et al.* Untargeted metabolomics identifies potential hypertrophic cardiomyopathy biomarkers in carriers of MYBPC3 founder variants. *Int J Mol Sci* 2023; **24**:4301. doi:10.3390/jms24044031
  31. Schuldt M, van Driel B, Algül S, Parbhudayal RY, Barge-Schaapveld DQCM, Güçlü A, *et al.* Distinct metabolomic signatures in preclinical and obstructive hypertrophic cardiomyopathy. *Cells* 2021; **10**:2950. doi:10.3390/cells10112950
  32. Ranjbarvaziri S, Kooiker KB, Ellenberger M, Fajardo G, Zhao M, Vander Roest AS, *et al.* Altered cardiac energetics and mitochondrial dysfunction in hypertrophic cardiomyopathy. *Circulation* 2021; **144**:1714-1731. doi:10.1161/CIRCULATIONAHA.121.053575
  33. Joshua J, Caswell J, O'Sullivan ML, Wood G, Fonfara S. Feline myocardial transcriptome in health and in hypertrophic cardiomyopathy—A translational animal model for human disease. *PLoS ONE* 2023; **18**:e0283244. doi:10.1371/journal.pone.0283244
  34. Jiwanonant P, Roytrakul S, Thaisakun S, Sukumolanan P, Petchdee S. Investigation of coagulation and proteomics profiles in symptomatic feline hypertrophic cardiomyopathy and healthy control cats. *BMC Vet Res* 2024; **20**:292. doi:10.1186/s12917-024-04170-0
  35. Liu M, Eckersall PD, Mrljak V, Horvatic A, Guillemin N, Galan A, *et al.* Novel biomarkers in cats with congestive heart failure due to primary cardiomyopathy. *J Proteomics* 2020; **226**:103896. doi:10.1016/j.jprot.2020.103896
  36. Kittleston MD, Meurs KM, Harris SP. The genetic basis of hypertrophic cardiomyopathy in cats and humans. *J Vet Cardiol* 2015; **17**:S53-S73. doi:10.1016/j.jvc.2015.03.001
  37. Meurs KM, Sanchez X, David RM, Bowles NE, Towbin JA, Reiser PJ, *et al.* A cardiac myosin binding protein C mutation in the Maine Coon cat with familial hypertrophic cardiomyopathy. *Hum Mol Genet* 2005; **14**:3587-3593. doi:10.1093/hmg/ddi386
  38. Meurs KM, Norgard MM, Ederer MM, Hendrix KP, Kittleston MD. A substitution mutation in the myosin binding protein C gene in ragdoll hypertrophic cardiomyopathy. *Genomics* 2007; **90**:261-264. doi:10.1016/j.ygeno.2007.04.007
  39. Freeman LM, Rush JE, Stern JA, Huggins GS, Maron MS. Feline hypertrophic cardiomyopathy: a spontaneous large animal model of human HCM. *Cardiol Res* 2017; **8**:139-142. doi:10.14740/cr578w
  40. Ford L, Kennedy AD, Goodman KD, Pappan KL, Evans AM, Miller LAD, *et al.* Precision of a clinical metabolomics profiling platform for use in the identification of inborn errors of metabolism. *J Appl Lab Med* 2020; **5**:342-356. doi:10.1093/jalm/jfz026
  41. Li Q, Laflamme DP, Bauer JE. Serum untargeted metabolomic changes in response to diet intervention in dogs with preclinical myxomatous mitral valve disease. *PLoS ONE* 2020; **15**:e0234404. doi:10.1371/journal.pone.0234404

42. Benjamini Y, Hochberg Y. Controlling the false discovery rate: a practical and powerful approach to multiple testing. *J R Stat Soc Ser B* 1995;**57**:289-300. doi:10.1111/j.2517-6161.1995.tb02031.x
43. Yang JJ, Shu XO, Herrington DM, Moore SC, Meyer KA, Ose J, et al. Circulating trimethylamine N-oxide in association with diet and cardiometabolic biomarkers: an international pooled analysis. *Am J Clin Nutr* 2021;**113**:1145-1156. doi:10.1093/ajcn/nqaa430
44. McDonald J. *Handbook of biological statistics*. 3rd ed. Baltimore (MD): Sparky House Publishing; 2014:254-260.
45. Kerner J, Hoppel C. Fatty acid import into mitochondria. *Biochim Biophys Acta* 2000;**1486**:1-17. doi:10.1016/s1388-1981(00)00044-5
46. Violante S, IJlst L, Te Brinke H, Koster J, Tavares de Almeida I, Wanders RJ, et al. Peroxisomes contribute to the acylcarnitine production when the carnitine shuttle is deficient. *Biochim Biophys Acta* 2013;**1831**:1467-1474. doi:10.1016/j.bbali.2013.06.007
47. Ljungvall I, Höglund K, Lilliehöök I, Oyama MA, Tidholm A, Tvedten H, et al. Serum serotonin concentration is associated with severity of myxomatous mitral valve disease in dogs. *J Vet Intern Med* 2013;**27**:1105-1112. doi:10.1111/jvim.12137
48. Blanco A, Blanco G. Chapter 11—membranes. In: Blanco A, Blanco G, eds. *Medical biochemistry*. Second Edition: Academic Press; 2022:233-279.
49. Blanco A, Blanco G. Chapter 5 - Lipids. In: Blanco A, Blanco G, eds. *Medical biochemistry*. Second Edition: Academic Press; 2022:105-129.
50. Slotte JP. Biological functions of sphingomyelins. *Prog Lipid Res* 2013;**52**:424-437. doi:10.1016/j.plipres.2013.05.001
51. Abbas R, Kombu RS, Ibarra RA, Goyal KK, Brunengraber H, Sanabria JR. The dynamics of glutathione species and ophthalmate concentrations in plasma from the VX2 rabbit model of secondary liver tumors. *HPB Surg* 2011;**2011**:709052. doi:10.1155/2011/709052
52. Kombu RS, Zhang GF, Abbas R, Mieyal JJ, Anderson VE, Kelleher JK, et al. Dynamics of glutathione and ophthalmate traced with 2H-enriched body water in rats and humans. *Am J Physiol Endocrinol Metab* 2009;**297**:E260-E269. doi:10.1152/ajpendo.00080.2009
53. Soga T, Baran R, Suematsu M, Ueno Y, Ikeda S, Sakurakawa T, et al. Differential metabolomics reveals ophthalmate as an oxidative stress biomarker indicating hepatic glutathione consumption. *J Biol Chem* 2006;**281**:16768-16776. doi:10.1074/jbc
54. Dello SA, Neis EP, de Jong MC, van Eijk HM, Kicken CH, Olde Damink SW, et al. Systematic review of ophthalmate as a novel biomarker of hepatic glutathione depletion. *Clin Nutr* 2013;**32**:325-330. doi:10.1016/j.clnu.2012.10.008
55. Gall WE, Beebe K, Lawton KA, Adam KP, Mitchell MW, Nakhle PJ, et al. Alpha-hydroxybutyrate is an early biomarker of insulin resistance and glucose intolerance in a nondiabetic population. *PLoS ONE* 2010;**5**:e10883. doi:10.1371/journal.pone.0010883
56. Pelletier G. Chapter 11—steroidogenic enzymes in the brain: morphological aspects. In: Martini L, ed. *Progress in brain research*. Vol.181. Elsevier; 2010:193-207. doi:10.1016/S0079-6123(08)81011-4
57. Li Q. Metabolic reprogramming, gut dysbiosis, and nutrition intervention in canine heart disease. *Front Vet Sci* 2022;**9**:791754. doi:10.3389/fvets.2022.791754
58. Knottnerus SJG, Bleeker JC, Wüst RCI, Ferdinandusse S, IJlst L, Wijburg FA, et al. Disorders of mitochondrial long-chain fatty acid oxidation and the carnitine shuttle. *Rev Endocr Metab Disord* 2018;**19**:93-106. doi:10.1007/s11154-018-9448-1
59. Vishwanath VA. Fatty acid beta-oxidation disorders: a brief review. *Ann Neurosci* 2016;**23**:51-55. doi:10.1159/000443556
60. Wajner M, Amaral AU. Mitochondrial dysfunction in fatty acid oxidation disorders: insights from human and animal studies. *Biosci Rep* 2016;**36**:e00281. doi:10.1042/BSR20150240
61. Guerra IMS, Ferreira HB, Melo T, Rocha H, Moreira S, Diogo L, et al. Mitochondrial fatty acid beta-oxidation disorders: from disease to lipidomic studies—a critical review. *Int J Mol Sci* 2022;**23**:13933. doi:10.3390/ijms232213933
62. Costa CG, Dorland L, Holwerda U, Tavares de Almeida I, Poll-The BT, Jakobs C, et al. Simultaneous analysis of plasma free fatty acids and their 3-hydroxy analogs in fatty acid beta-oxidation disorders. *Clin Chem* 1998;**44**:463-471. doi:10.1093/clinchem/44.3.463
63. Adams SH, Hoppel CL, Lok KH, Zhao L, Wong SW, Minkler PE, et al. Plasma acylcarnitine profiles suggest incomplete long-chain fatty acid beta-oxidation and altered tricarboxylic acid cycle activity in type 2 diabetic African-American women. *J Nutr* 2009;**139**:1073-1081. doi:10.3945/jn.108.103754
64. Spiekerkoetter U, Sun B, Zytkevich T, Wanders R, Strauss AW, Wendel U. MS/MS-based newborn and family screening detects asymptomatic patients with very-long-chain acyl-CoA dehydrogenase deficiency. *J Pediatr* 2003;**143**:335-342. doi:10.1067/S0022-3476(03)00292-0
65. Shekhawat PS, Matern D, Strauss AW. Fetal fatty acid oxidation disorders, their effect on maternal health and neonatal outcome: impact of expanded newborn screening on their diagnosis and management. *Pediatr Res* 2005;**57**:78R-86R. doi:10.1203/01.PDR.0000159631.63843.3E
66. Murashige D, Jang C, Neinast M, Edwards JJ, Cowan A, Hyman MC, et al. Comprehensive quantification of fuel use by the failing and nonfailing human heart. *Science* 2020;**370**:364-368. doi:10.1126/science.abc8861
67. Lommi J, Kupari M, Koskinen P, Näveri H, Leinonen H, Pulkki K, et al. Blood ketone bodies in congestive heart failure. *J Am Coll Cardiol* 1996;**28**:665-672. doi:10.1016/0735-1097(96)00214-8
68. Lommi J, Kupari M, Yki-Jarvinen H. Free fatty acid kinetics and oxidation in congestive heart failure. *Am J Cardiol* 1998;**81**:45-50. doi:10.1016/s0002-9149(97)00804-7
69. Lommi J, Koskinen P, Näveri H, Harkonen M, Kupari M. Heart failure ketosis. *J Intern Med* 1997;**242**:231-238. doi:10.1046/j.1365-2796.1997.00187.x
70. Flam E, Jang C, Murashige D, Yang Y, Morley MP, Jung S, et al. Integrated landscape of cardiac metabolism in end-stage human nonischemic dilated cardiomyopathy. *Nat Cardiovasc Res* 2022;**1**:817-829. doi:10.1038/s44161-022-00117-6
71. Brody TOM. 4—Regulation of energy metabolism. In: Brody TOM, ed. *Nutritional Biochemistry*. Second ed. San Diego: Academic Press; 1999:157-271.
72. Li Q, Larouche-Lebel E, Loughran KA, Huh TP, Suchodolski JS, Oyama MA. Metabolomics analysis reveals deranged energy metabolism and amino acid metabolic reprogramming in dogs with myxomatous mitral valve disease. *J Am Heart Assoc* 2021;**10**:e018923. doi:10.1161/JAHA.120.018923
73. Neubauer S, Horn M, Cramer M, Harre K, Newell JB, Peters W, et al. Myocardial phosphocreatine-to-ATP ratio is a predictor of mortality in patients with dilated cardiomyopathy. *Circulation* 1997;**96**:2190-2196. doi:10.1161/01.cir.96.7.2190
74. Magni G, Amici A, Emanuelli M, Raffaelli N, Ruggieri S. Enzymology of NAD+ synthesis. In: *Advances in enzymology and related areas of molecular biology: mechanism of enzyme action, part A*. Vol.73; 1999:135-182. doi:10.1002/9780470123195.ch5
75. Membrez M, Migliavacca E, Christen S, Yaku K, Trieu J, Lee AK, et al. Trigonelline is an NAD(+) precursor that improves muscle function during ageing and is reduced in human sarcopenia. *Nat Metab* 2024;**6**:433-447. doi:10.1038/s42255-024-00997-x
76. Elia M. Organ and tissue contribution to metabolic rate. In: Kinney JM, Tucker HN, eds. *Energy metabolism: tissue determinants and cellular correlates*. Raven Press, New York; 1992:61-79.
77. Mari M, Morales A, Colell A, García-Ruiz C, Kaplowitz N, Fernández-Checa JC. Mitochondrial glutathione: features, regulation and role in disease. *Biochim*

- Biophys Acta* 2013;**1830**:3317-3328. doi:10.1016/j.bbagen.2012.10.018
78. Schomakers BV, Jillings SL, van Weeghel M, Vaz FM, Salomons GS, Janssens GE, *et al.* Ophthalmic acid is a glutathione regulating tripeptide. *FEBS J* 2024;**291**:3317-3330. doi:10.1111/febs.17061
  79. Teskey G, Abraham R, Cao R, Gyurjian K, Islamoglu H, Lucero M, *et al.* Glutathione as a marker for human disease. *Adv Clin Chem* 2018;**87**:141-159. doi:10.1016/bs.acc.2018.07.004
  80. Giustarini D, Milzani A, Dalle-Donne I, Rossi R. How to increase cellular glutathione. *Antioxid (Basel)* 2023;**12**:1094. doi:10.3390/antiox12051094
  81. Vanholder R, Argilés A, Baurmeister U, Brunet P, Clark W, Cohen G, *et al.* Uremic toxicity: present state of the art. *Int J Artif Organs* 2001;**24**:695-725. doi:10.1177/039139880102401004
  82. Vanholder R, De Smet R, Glorieux G, Argilés A, Baurmeister U, Brunet P, *et al.* Review on uremic toxins: classification, concentration, and interindividual variability. *Kidney Int* 2003;**63**:1934-1943. doi:10.1046/j.1523-1755.2003.00924.x
  83. Fine RN, Nissenson AR. In: Nissenson AR, Fine RN, eds. *Handbook of dialysis therapy*. Fourth ed. Philadelphia: Saunders/Elsevier; 2008.
  84. Houang EM, Bartos J, Hackel BJ, Lodge TP, Yannopoulos D, Bates FS, *et al.* Cardiac muscle membrane stabilization in myocardial reperfusion injury. *JACC Basic Transl Sci* 2019;**4**:275-287. doi:10.1016/j.jacbts.2019.01.009
  85. Kano K, Aoki J, Hla T. Lysophospholipid mediators in health and disease. *Annu Rev Pathol* 2022;**17**:459-483. doi:10.1146/annurev-pathol-050420-025929
  86. Vecchini A, Del Rosso F, Binaglia L, Dhalla NS, Panagia V. Molecular defects in sarcolemmal glycerophospholipid subclasses in diabetic cardiomyopathy. *J Mol Cell Cardiol* 2000;**32**:1061-1074. doi:10.1006/jmcc.2000.1140
  87. Karliner JS. Lysophospholipids and the cardiovascular system. *Biochim Biophys Acta* 2002;**1582**:216-221. doi:10.1016/s1388-1981(02)00174-9
  88. Kolesnick RN. Sphingomyelin and derivatives as cellular signals. *Prog Lipid Res* 1991;**30**:1-38. doi:10.1016/0163-7827(91)90005-p
  89. Kikas P, Chalikias G, Tziakas D. Cardiovascular implications of sphingomyelin presence in biological membranes. *Eur Cardiol* 2018;**13**:42-45. doi:10.15420/eccr.2017:20:3
  90. Preveden A, Golubovic M, Bjelobrk M, Miljkovic T, Ilic A, Stojic S, *et al.* Gender related differences in the clinical presentation of hypertrophic cardiomyopathy-an analysis from the SILICOFCM database. *Medicina (Kauņas)* 2022;**58**:314. doi:10.3390/medicina58020314
  91. Olivetto I, Maron MS, Adabag AS, Casey SA, Vargiu D, Link MS, *et al.* Gender-related differences in the clinical presentation and outcome of hypertrophic cardiomyopathy. *J Am Coll Cardiol* 2005;**46**:480-487. doi:10.1016/j.jacc.2005.04.043
  92. Granström S, Godiksen MT, Christiansen M, Pipper CB, Willesen JL, Koch J. Prevalence of hypertrophic cardiomyopathy in a cohort of British shorthair cats in Denmark. *J Vet Intern Med* 2011;**25**:866-871. doi:10.1111/j.1939-1676.2011.0751.x
  93. Rush JE, Freeman LM, Fenollosa NK, Brown DJ. Population and survival characteristics of cats with hypertrophic cardiomyopathy: 260 cases (1990-1999). *J Am Vet Med Assoc* 2002;**220**:202-207. doi:10.2460/javma.2002.220.202
  94. Payne J, Luis Fuentes V, Boswood A, Connolly D, Koffas H, Brodbelt D. Population characteristics and survival in 127 referred cats with hypertrophic cardiomyopathy (1997 to 2005). *J Small Anim Pract* 2010;**51**:540-547. doi:10.1111/j.1748-5827.2010.00989.x